Efficiency Evaluation of a Matrix Converter with a Boost-up AC Chopper in Adjustable Drive System

Kazuhiro Koiwa* Jun-ichi Itoh*

*Nagaoka University of Technology

Abstract:- In this paper, the validity of the proposed circuit which consist of a V-connection AC chopper and a matrix converter is evaluated in an IPMSM adjustable speed drive system in term of efficiency using loss calculations and experiments. As a result, it is confirmed that the total efficiency of the proposed system can achieve 79.7%. Furthermore, it is revealed that the proposed system is effectiveness when the input line voltage is 93.5% lower than the motor rated voltage.

Keywords : Matrix converter, V-connection AC chopper, Flux-weakening control, IPM motor

1. Introduction

A matrix converter (MC) which can convert an AC power supply voltage directly into an AC output voltage of variable amplitude and frequency without the large energy storages, such as electrolytic capacitors, have been actively studied recently [1-5]. However, one of the disadvantages of the MC is that the voltage transfer ratio, which defines as the ratio between the output voltage and the input voltage, is constrained to 0.866. As a result, in the adjustable speed drive system, due to implementation of flux-weakening control the motor loss increases inherently.

The authors previously proposed a circuit topology which connects a V-connection AC chopper in the input stage of the MC that enables boost-up functionality [2-3]. However, additional loss from the AC chopper occurs in the proposed circuit structure. Thus, in comparison with the conventional MC, the efficiency of the proposed circuit is lower due to the additional chopper loss.

In this paper, the validity of the proposed circuit is evaluated in the adjustable speed drive system in order to clarify the advantage of the proposed system. At first, the chopper loss in the proposed circuit and the copper loss of the motor in the conventional MC are introduced theoretically. Then, the difference between the chopper loss and the copper loss are compared, where flux-weakening control is implemented in the motor control. Finally, the operation of the proposed system will be demonstrated as a 3.7-kW Interior Permanent Magnet motor (IPM motor). In addition, the chopper loss and the copper loss are evaluated to clarify the validity of the proposed system.

2. Circuit topology and Chopper losses

Fig.1 shows the proposed circuit which connects a V-connection AC chopper in the input stage of the MC. Note that the virtual indirect control method is applied in the MC [4]. Eight IGBTs are used in the AC chopper. The relationship between the input voltage v_{in} and the output voltage v_{out} is expressed by

$$v_{out} = \beta \cdot \lambda_{mc} \cdot v_{in} \quad \text{.....(1),}$$

where, λ_{mc} is the modulation index of the MC, β is the boost-up ratio of the chopper and v_{in} is the input voltage. Basically, the function of the AC chopper is to boost-up the input voltage. Feedback control is not required for the filter capacitor since both the input and output sides of the AC chopper are AC voltage.

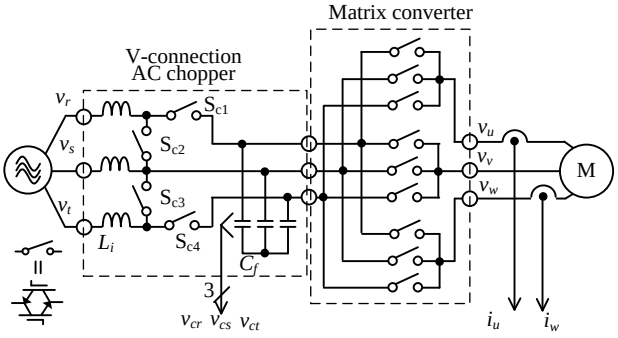

Fig. 1. Circuit configuration of proposed circuit.

Therefore, the capacitor value does not dominate by the voltage control response and the current response from the input side, which is contrast to a BTB system. As a result, the V-connection AC chopper and its components do not dominate the size and the weight in comparison to the origin structure of a MC. In addition, the maximum output voltage of the proposed circuit is decided by the duty ratio of the AC chopper. It should be noted that the switches in the AC chopper do not operate when the voltage transfer ratio is lower than 0.866 of the input voltage. That is, in the range of low output voltage, the V-connection AC chopper in the proposed circuit does not generate the switching loss in low output voltage.

However, the conduction loss occurs in the AC chopper even switching operation is disabled. Therefore, it is concerned that the conversion efficiency is degraded by adding the AC chopper.

2.1 Conduction loss

In order to consider the influence of the chopper loss for the proposed circuit, the chopper losses such as the conduction loss and the switching loss are theoretically derived in this section.

At first, the conduction loss of S_{c1} is expressed by (2).

$$P_{conS1} = \frac{1}{\pi}\int_0^{\pi} v_{ce} i_r \, d\omega t \quad \text{.....(2)}$$

where, v_{ce} is the on-state voltage of S_{c1} which is expressed by (3) and i_r is the input current.

$$v_{ce} = k_{con1} i_r + k_{con2} \quad \text{.....(3)}$$

Note that k_{con1} and k_{con2} are defined from the on-state voltage characteristics in the datasheet of the switching device. In this paper, SK80GM063 which is in SEMIKRON is used as the chopper device. The rated voltage and the rated current of this

IGBT are 600 V and 81 A, respectively. From these equation, the conduction loss of S_{c1} is introduced by (4).

$$P_{con\_S1} = \frac{k_{con1}}{\beta} I_{in}{}^2 + \frac{2\sqrt{2}}{\pi} \frac{k_{con2}}{\beta} I_{in} \quad \text{.....(4)}$$

where, I_{in} is the effective value of the input current. In similarly, the conduction loss of S_{c2} is expressed by (5).

$$P_{con\_S2} = \frac{(\beta-1)k_{con1}}{\beta} I_{in}{}^2 + \frac{2\sqrt{2}}{\pi} \frac{(\beta-1)k_{con2}}{\beta} I_{in} \quad \text{.....(5)}$$

2.2 Switching loss

The switching loss of the AC chopper is obtained by the input line voltage v_{rs} and the input current i_{in}. Thus, the switching loss P_{ton_s1} and P_{ton_s2} are expressed by (6) and (7), respectively.

$$P_{ton\_S1} = \frac{1}{\pi} \int_{\frac{5}{6}\pi}^{\pi} E_{on} f_s \frac{v_{rs}}{V_s} d\omega t$$
$$= \frac{\sqrt{2} V_{in} f_s}{24\pi V_s} (\beta-1)[(\sqrt{6}\pi - 6)k_{ton1} I_{in} + 12(\sqrt{3}-2)k_{ton2}]$$

.....(6)

$$P_{ton\_S2} = \frac{1}{\pi} \int_{\frac{\pi}{6}}^{\pi} E_{on} f_s \frac{v_{rs}}{V_s} d\omega t$$
$$= \frac{\sqrt{2}\beta V_{in} f_s}{24\pi V_s} [(5\sqrt{6}\pi + 3\sqrt{2})k_{ton1} I_{in} + 12(1+\sqrt{3})k_{ton2}]$$

.....(7)

where, E_{on} is the instant switching loss which is shown by (8).

$$E_{on} = k_{ton1} i_{in} + k_{ton2} \quad \text{.....(8)}$$

Note that k_{ton1} and k_{ton2} are defined from the switching loss characteristics in the datasheet of the switching device.

Fig. 2 shows the conduction and switching losses of the AC chopper by the theoretical calculation and the simulation. Note that the chopper loss of the calculation results is the sum of the equations of (4), (5), (6) and (7). Additionally, k_{con1} and k_{con2} are 0.0182 and 0.9773, respectively. On the other hand, k_{ton1} and k_{ton2} are 0.00005 and 0.0, respectively. These parameters were obtained from the datasheet of the switching devices. As the result, the calculation results are corresponding to the simulation results. Thus, the validity of the derived equations of the chopper loss is confirmed.

3. Relationship flux-weakening control to copper loss

In order to drive an IPM motor in high rotating speed area within the output voltage limitation of the MC, the flux-weakening control is necessary to apply in the MC control. This is because the back electromotive force becomes higher with increasing the rotating speed. The output voltage which is necessary to drive the motor can be degraded by the flux-weakening control. There, the d-axis current i_d for the flux-weakening control is introduced.

Fig. 3 shows the phasor vector diagram of the flux-weakening control where e_q is the back electromotive force, v and v' are the terminal voltage in the IPM motor without the field-weakening control and with the field-weakening control, respectively. Field-weakening control in the IPM motor can equally weaken the magnetic flux in the permanent magnet from the d axis armature magnetic flux. As a result, the rotation speed area can be extended by implementing the field-weakening control. From the Fig. 3, it

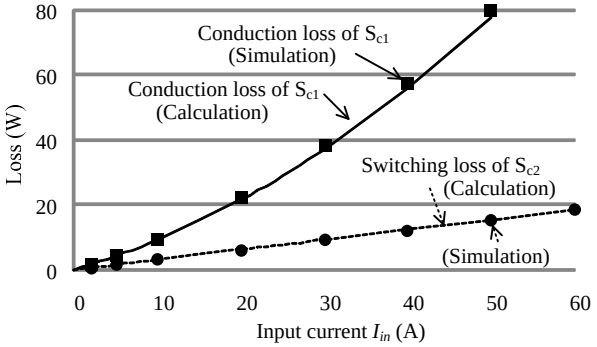

Fig. 2. Chopper loss by simulation result.

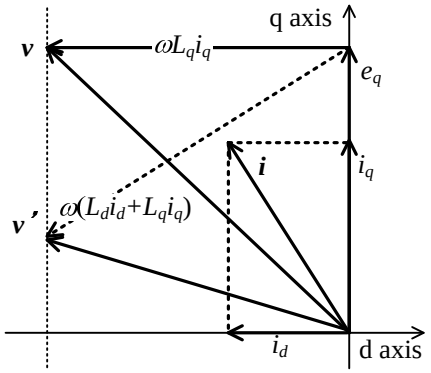

Fig. 3. Phasor vector diagram on flux-weakening control.

is expressed by (9).

$$V_{om} = \sqrt{v_d{}^2 + v_q{}^2}$$
$$= \sqrt{(\omega L_q i_q)^2 + (\omega L_d i_d + e_q)^2} \quad \text{.....(9)}$$

where, V_{om} is the limitation of the output phase voltage that the MC can output. Therefore, the d-axis current in the flux-weakening control is calculated by (10).

$$i_d = \frac{-e_q + \sqrt{V_{om}{}^2 - (\omega L_q i_q)^2}}{\omega L_d} \quad \text{.....(10)}$$

The motor current is increased due to the flux-weakening control. As a result, the motor loss and the converter loss will be increased. In order to validate the AC chopper, the copper loss which is increased by the flux-weakening control is introduced. In other words, the equation of the copper loss that subjects to the input line voltage is calculated.

At first, the torque of an IPM motor is expressed by

$$T = P_n[\frac{e_q}{\omega} i_q + (L_d - L_q) i_d i_q] \quad \text{.....(11),}$$

where, P_n is the number of pole.

Thus, V_{om} is expressed by (12) from (10) and (11).

$$V_{om} = \sqrt{[\frac{L_d}{(L_d - L_q)}(\frac{\omega T}{P_n} - \frac{L_q}{L_d} e_q i_q)\frac{1}{i_q}]^2 + (\omega L_q i_q)^2} \quad \text{....(12)}$$

Note that the q-axis current should be obtained to derive the copper loss. However, Eq. (12) cannot obtain the q-axis current. For this reason, the q-axis current is calculated by numerical analysis. It should be noted that the q-axis current is limited by (13).

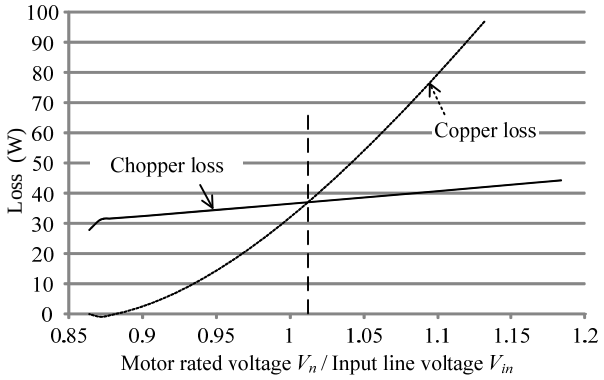

Fig. 4. Comparison between experiment and calculation.

Table 1. Motor parameters.

Rated mechanical power P_m	3.7 kW	Winding resistance R_w	0.693 Ω
Back electromotive force e_q	151 V	d axis inductance L_d	6.2 mH
Rated voltage V_n	180 V	q axis inductance L_q	15.3 mH
Rated current I_n	14 A	Inertia moment J	0.0212 kgm^2
Synchronous speed ω_s	1800 rpm	Number of pole pairs P_n	3
Rated torque T_{eR}	19.6 Nm		

Table 2 Experimental conditions.

Rotating speed ω		1800 rpm	Output control	Vector control
Input frequency		50 Hz	Commutation	Voltage-type
Carrier frequency	Chopper	10 kHz	MC control	Virtual indirect control
	MC			
Response angular frequency ω_r	ACR	3000 rad/s	Load	3.7-kW IPM motor
	ASR	200 rad/s		
Input reactor L_i		2 mH	Switch of MC	1MBI100W-120A
Filter capacitor C_f		14.2 μF	Switch of chopper	SK80GM063
Damping resistor R_d (Conventional MC)		32.7 Ω		

$$\left|i_q\right| \le \frac{V_{om}}{\omega L_q} \quad \text{.....(13)}$$

On the other hand, d-axis current can be calculated by (10). Therefore, the copper loss P_c is expressed by (14).

$$P_c = 3R_w I_o^{\,2} = 3 \cdot R_w \cdot \frac{(i_d^{\,2} + i_q^{\,2})}{2} \quad \text{.....(14)}$$

where, R_w is the primary wire resistance of the IPM motor. In addition, I_o is the effective value of the output current.

Fig. 4 shows the calculation result of the chopper loss and the copper loss. Note that the copper loss was calculated by the motor parameter which is shown in Table 1. Since, the flux-weakening control in the IPM motor is not capable of wide range of application. Therefore, in order to extend the applications, the input voltage of the proposed circuit and the conventional MC are degraded. Then, high rotating speed of the IPM motor is possible to be simulated. According to the result, in case that ratio between motor rated voltage V_n and input voltage V_{in} (V_n/V_{in}) is less than 1.01 p.u., the chopper loss is larger than the copper loss. On the other hand, as V_n/V_{in} is higher than 1.01 p.u., the chopper loss is less than the copper loss. This is because the motor current and the copper loss are increased with the ratio of V_n/V_{in}.

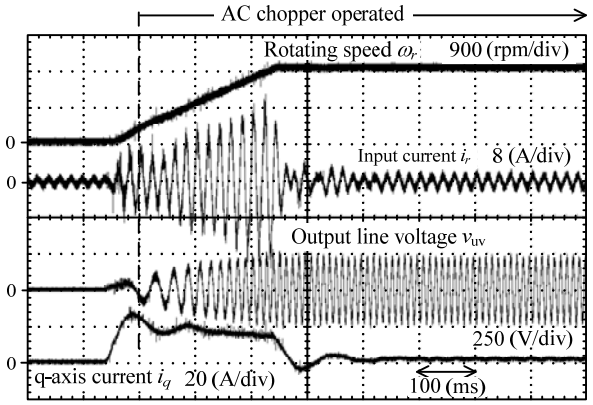

Fig. 5 Acceleration test.

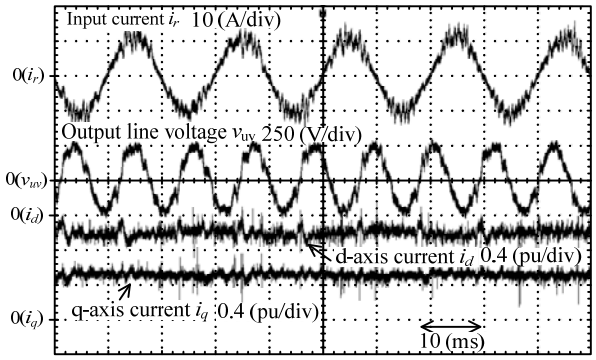

Fig. 6. Experimental results in motor-load.

4. Experimental results

Fig. 5 shows the acceleration tests for the IPM motor which is driven by the proposed circuit with vector control. Table 2 shows the experimental parameters. In Fig. 5, the AC chopper starts operating while the rotating speed command ω^* is over 0.2pu because the harmonic distortion is decreased by the damping control. Additionally, it is confirmed that the input and q-axis current are not drastically changed because of the operation of AC chopper. Therefore, the proposed circuit can improve the transfer ratio of the MC.

Fig. 6 shows the experimental results at rated rotating speed. Note that the torque is 85%. In addition, the damping control is applied in the AC chopper [5]. According to the waveform, it is confirmed that the total harmonic distortion (THD) of the input current is 12.2%. In order to reduce the THD, it is necessary to optimize the damping gain.

Fig. 7 shows the output line voltage characteristic based on the mechanical output power. The rated line voltage of the IPM motor V_n is 180V. Thus, the output line voltage is limited up to 180V by the flux-weakening control. According to the result, it is confirmed that the output line voltage is limited up to 180V by the flux-weakening control. Thus, the flux-weakening control is validated by experimental results. Moreover, as the mechanical output power is over 1400 W, d-axis current become larger due to the flux-weakening control. As a result, the copper loss is increased due to flux-weakening control.

Fig. 8 shows the total efficiency, which is included the converter efficiency and the motor efficiency, proportional to the mechanical output power. In addition, the motor efficiency is calculated from the rotating speed and the estimated torque. As a result, it is

confirmed that the total efficiency is 79.7% in 2200-W load.

Fig. 9 shows the input current THD characteristic of the converter. Note that the damping control is applied in the AC chopper in all of area. According to the result, it is confirmed that the input current THD is over 8%. In other words, the input filter resonance cannot be suppressed by the damping control. This is because the damping gain is not optimized.

Fig. 10 shows the total loss comparison between the calculation results and the experimental results. Note that the input voltage V_{in} was changed. Additionally, the iron loss and the mechanical loss were obtained from experiment. Accordingly, the total efficiency of the conventional MC which applied the flux-weakening control becomes low as the input line voltage decreased. This is because the conduction loss of the converter and the primary order copper loss of the IPM motor are becoming larger due to the flux-weakening control.

On the other hand, the AC chopper in the proposed circuit can improve the input line voltage which has been decreased. Thus, the flux-weakening control is not necessary to apply in the proposed circuit. For this reason, high efficiency of the proposed circuit can be achieved.

In the calculation and experimental results, in case that the ratio of input line voltage and motor rated voltage is over 1.07 p.u. , the total loss of the proposed system is less than that of the conventional MC. However, in comparison with Fig. 4, there is the different the turning point. This is because the iron loss and mechanical loss is not allowed in Fig. 4. The iron loss is depending on the output line voltage and frequency. Therefore, the validity of the proposed system can be revealed as the input line voltage is 93.5% lower than the motor rated voltage.

5. Conclusion

In this paper, the validity of the proposed circuit is evaluated in term of the efficiency in an IPM motor drive system. Consequently, the chopper loss and the copper loss are derived theoretical and simulation. As a result, the effective area that the chopper loss is less than the copper loss is confirmed.

The chopper loss and the copper loss were demonstrated by a 3.7-kW IPM motor. As a result, it was confirmed that the total efficiency of the proposed system was 79.7% in 2200-W load. Moreover, it can be accomplished that the validity of the proposed system is confirmed as the input voltage is 93.5% lower than the motor rated voltage.

In future works, the damping gain will be optimized. Moreover, the harmonic distortion in the input current will be suppressed.

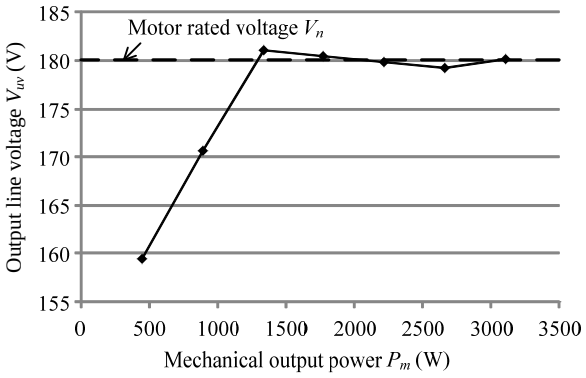

Fig. 7. Output line voltage characteristic.

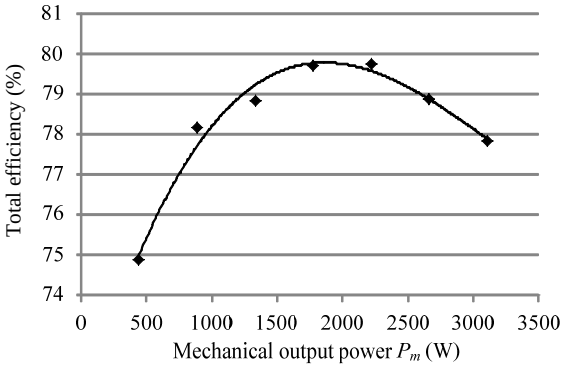

Fig. 8. Total efficiency characteristic.

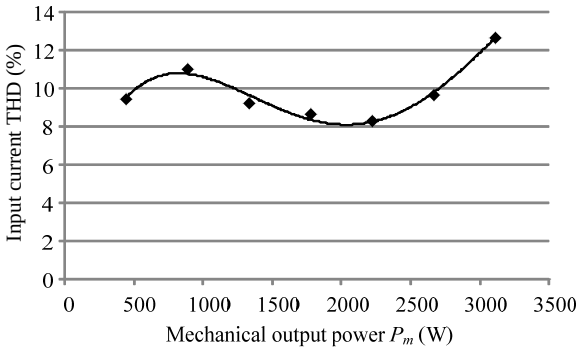

Fig. 9. Input current THD characteristic.

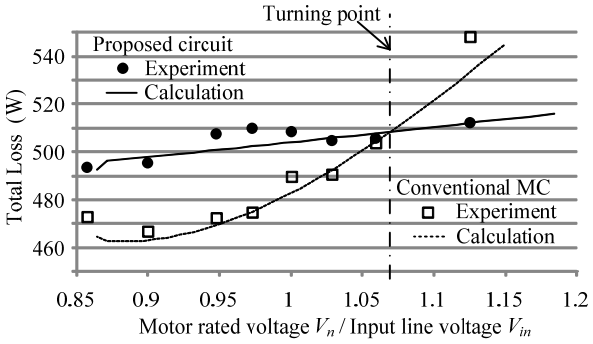

Fig. 10. Total loss comparison between calculation results and experimental results.

References

[1] P. W. Wheeler, J. Rodriguez, J. C. Clare, L. Empringham: "Matrix Converters: A Technology Review", IEEJ Trans. D, Vol. 49, No. 2, pp. 274-288 (2002)

[2] K. Koiwa, J. Itoh: "Verification of Effectiveness of a Matrix Converter with Boost-up AC Chopper by Using an IPM Motor", The Applied Power Electronics Conference and Exposition 2012, Vol. , No. 2265, pp. 1178-1184 (2012)

[3] Z. Fedyczak, P. Szczesniak, M. Klytta: "Matrix-Reactance Frequency Converter Based on Buck-Boost Topology", EPE-PEMC 2006, Vol. , No. , pp. 763-768 (2006)

[4] J. Itoh, H. Kodachi, A. Odaka, I. Sato, H. Ohguchi, H. Umida: "A High Performance Control Method for the Matrix Converter Based on PWM generation of Virtual AC/DC/AC Conversion", JIASC IEEJ, Vol. , No. , pp. I-303-I-308 (2004)

[5] K. Koiwa, J. Itoh: "A damping control method for a matrix converter with a boost-up AC chopper ", Power Electronics and Motion Control Conference (IPEMC), 2012 7th International , Vol. 2, No. , pp. 783-789 (2012)